Progress In Electromagnetics Research C, Vol. 38, 205–216, 2013

GUIDED- AND RADIATED-WAVE CHARACTERISTICS OF A RECTANGULAR PATCH ANTENNA LOCATED ON A SINGLY-CURVED SURFACE

Keyhan Hosseini and Zahra Atlasbaf *

Faculty of Engineering, Department of Electrical and Computer Engineering, Tarbiat Modares University (TMU), Tehran, Iran

Abstract—A modified Schwarz-Christoffel transformation (SCT) is used to obtain guided- and radiated-wave characteristics of a singly-curved rectangular patch antenna. The method is to map a straight channel into an arbitrarily-curved channel. This simplifies the problem to that of a planar rectangular patch antenna. Applying conventional SCT to the problem confronts two difficulties: the region under investigation is elongated, and it has curved boundaries. Therefore, SCT is modified to handle the problem. Input impedance, VSWR and radiation patterns of a conformal patch antenna on a parabolic surface are obtained utilizing the proposed SCT and either numerical or analytical treatment of a planar patch antenna, and the results are verified. Effect of parabolic curvature on the above-mentioned characteristics is investigated.

1. INTRODUCTION

Analysis and design of conformal antennas have been a subject of interest for years. The complexity of these antennas prevents them from having a closed form analytic formula, except for special structures [1–3]. Common full-wave methods such as MoM, FDTD and FEM widely apply to these structures [4–7]. However, these methods are generally very time-consuming and yield no physical insight into the problem.

Conformal mapping is a fast and powerful tool amongst many other tools to analyze conformal structures when it is applicable. In our previous work, we applied this method on a cylindrical leaky-wave antenna with circular cross-section to predict its scattering parameters

Received 17 November 2012, Accepted 26 March 2013, Scheduled 29 March 2013

* Corresponding author: Zahra Atlasbaf (atlasbaf@modares.ac.ir).

and radiation patterns [8]. However, that work was only useful for a circular cross-section. In this paper, a semi-analytic method (modified SCT) is developed to handle an arbitrary cross-section, and thereby to analyze and synthesize any singly-curved conformal antenna. Since this method is specifically designed to deal with conformal antennas, it makes some assumptions which lets the method be considerably fast and easy to formulate. Also, it depends only on the curved surface and not on the structure on it; therefore, SCT is run only once for a special curved surface, and the results can be tabulated to be applied on any other structure placed on that surface later. SCT links a conformal structure to a planar one whose analysis and design procedures are much faster and may have closed-form solutions. Reference [9] also deals with conformal structures; however, it is just an approximation and can't be used for rigorous scenarios. Reference [10] solves the conformal map from a closed curve to a circle. However, it deals with Symm's integral equation by solving a large system of equations, which is a time-consuming procedure even for simple shapes. Reference [11] applies conformal maps to elongated polygons with straight sides, but curved sides are not studied. That work is published in applied mathematics field. Reference [12] tries to generate suitable curved coordinates to be useful in solving fluid flow in those coordinates. However, no plan is devised to handle elongated regions. Reference [13] uses conformal mapping to map cylindrical and elliptic cross-sections into rectangles, whose method can't be generalized to analyze an arbitrary cross-section. Up to our knowledge, in microwave and antenna engineering no effort has been made to obtain electromagnetic characteristics of curved microstrip structures with arbitrary cross-section by the means of Schwarz-Christoffel transformation.

This paper is organized as follows: first, the problem of obtaining the guided- and radiated-wave characteristics of a patch antenna on a parabolic surface is proposed. Then, the basic theory of modified SCT is expressed. The modification is made in order to make SCT suitable to deal with curved boundaries and elongated regions. Finally, this method is applied to the main problem, and the results are verified by the means of CST full-wave simulator.

2. PROBLEM DESCRIPTION AND BASIC THEORY

2.1. Problem at Hand

Figure 1(a) shows a conformal patch antenna with a recessed microstrip line feed located on a singly-curved body. We assume that the substrate is a single-layer dielectric, and the ground and microstrip traces are

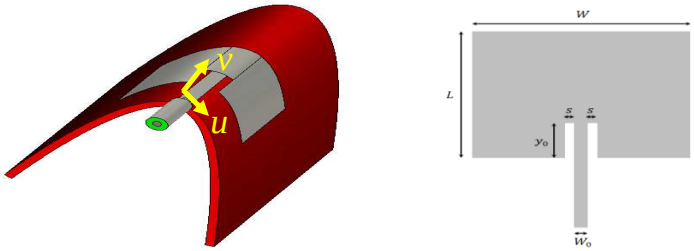

(a) (b)

Figure 1. (a) A recessed line fed patch antenna on a parabolic surface. (b) The patch and feed dimensions when exposed to no curvature.

PEC without any thickness. The goal is to obtain input impedance, VSWR and radiation patterns of this structure.

In this case, SCT is used as a conformal map $w = f(z)$ to map a planar structure into a curved one. Conformal maps preserve guided- and radiated-wave characteristics of a two dimensional structure working in TEM mode, in which the longitudinal component of the field is zero and hence Laplace's equation can be applied. Conformal maps preserve Laplace's equation. When only one mode propagates, microstrip structures with a dielectric other than air have a very small longitudinal field component which can be ignored. In this case, the working mode is called quasi-TEM and thereby, conformal mapping yields good approximations of the electromagnetic characteristics of the structure [14]. In this paper, we made sure that both conformal and planar antennas work in quasi-TEM mode at the desired frequencies using CST software facilities. The method is to monitor electric field components at some cross-sections of the feed and the patch, and to compare the longitudinal component of the field with transversal one. This was done for both conformal and planar mapped structures. We concluded that the mode is quasi-TEM when the transversal field was much larger (at least 10 times larger) than longitudinal field. Note that the patch antenna which works in TM_{010} mode, has very small longitudinal fields in the studied frequencies, whose mode of operation can also be considered quasi-TEM. Figure 1(b) shows the dimensions of the patch antenna when it is not exposed to any curvature. The proposed SCT generates a one-to-one function between points on the curved and planar bodies, in other words, by this method both SCT and inverse SCT are obtained. Hence, any segment on the curved boundary corresponds to a segment with a determined length on the planar one whose design is much easier and its simulation is much faster.

2.2. Modified SCT

SCT was originally utilized to map upper half plane into a polygon [15]. If the polygon has an elongation (Figure 2(a)), the points z_i (prevertices) in the z-plane which should be mapped to their corresponding points w_i in the w-plane may be too close to each other which can't be distinguished in any computer arithmetic system (crowding effect). If the shape to be mapped has an elongation too, the crowding effect may not happen. Elongated regions have large Aspect Ratios ($AR \gg 1$), whereas regions without any elongation have aspect ratios near to unity ($AR \approx 1$). Intuitively, crowding is a helpful concept but it is difficult to be defined precisely. *Roughly speaking*, the ratio of a length in w-plane to the corresponding length in z-plane is exponential when the shapes have very different ARs and it is linear when they have close ARs. In w-plane, assume a length that can be understood by a computer with a specific arithmetic precision. If the shape in w-plane is elongated and the shape in z-plane is not elongated, the two ARs are very different and the corresponding distance in z-plane may not be understood by that arithmetic precision since it is exponentially smaller than the distance in w-plane. Whereas, if both shapes are elongated the ARs can be close to each other and the corresponding length in z-plane is likely to be understood in that arithmetic precision. Although, it is not guaranteed that the crowding effect never occurs when both shapes have close ARs, practically it is a useful approach to circumvent crowding. For more details, see [11]. The cross-section of the configuration shown in Figure 1 can be assumed as an elongated

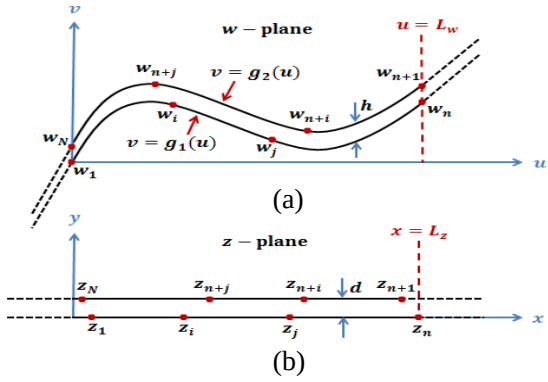

Figure 2. (a) A curved channel with elongated cross-section in w-plane. (b) A straight channel in z-plane which is mapped to the curved channel by SCT. In this paper, we assume that $d = h$.

curved rectangle. Here, we use an elongated straight planar *channel* extended from both sides to infinity in z-plane. To make the curved cross-section have the same *order of elongation* as that of the planar channel, we extend it linearly from both sides to infinity such that the lines are tangent to both ends of the curved structure, as shown in Figure 2(a). In this figure, the dashed lines are the line extensions. The SCT that maps a straight planar channel to a polygon channel with M straight sides, is as follows:

$$f(z) = A\int^{z}\prod_{i=1}^{M}\left(e^{\frac{\pi\xi}{d}} - e^{\frac{\pi z_i}{d}}\right)^{\alpha_i-1} d\left(e^{\frac{\pi\xi}{d}}\right) + B \tag{1}$$

$\pi(1-\alpha_i)$ is the interior angle of the vertex i in a counter-clockwise sense. A and B are two constants that determine the orientation and location of the polygon. Rearranging the factors yields [11]

$$f(z) = A\int^{z}\prod_{i=1}^{M}\left[\sinh\frac{\pi}{2d}(\xi - z_i)\right]^{\alpha_i-1} d\xi + B \tag{2}$$

This is a suitable formula to map a strip into a polygon with straight sides, however, the discussed configuration here is curved [12]. As M tends to infinity, we can rewrite (2) as

$$f(z) = A\int^{z}\exp\left(-\frac{1}{\pi}\int^{\theta}\ln\left(\sinh\frac{\pi}{2d}(\xi-\delta)\right)d\theta(\delta)\right)d\xi + B \tag{3}$$

where $\theta(\delta)$ is the change in the direction angle of the tangent to the curved channel boundary at the image point of the value δ. $\delta = x$ on the planar channel lower part and $\delta = x + id$ on the planar channel upper part.

2.3. Numerical Evaluation of Modified SCT

By decomposing the internal integration interval into N *suitably* small elements, we have:

$$f(z) = A\int^{z}\exp\left(-\frac{1}{\pi}\sum_{i=1}^{N}\int_{\theta_i}^{\theta_{i+1}}\ln\left(\sinh\frac{\pi}{2d}(\xi-\delta)\right)d\theta(\delta)\right)d\xi + B \tag{4}$$

By approximating θ as [12]

$$\theta_i = a_i\delta_i^2 + b_i\delta_i + c_i \tag{5}$$

Equation (4) can be written in the following form:

$$f(z) = A\int^{z}\sum_{i=1}^{N}\left[\sinh\frac{\pi}{2d}(\xi-\delta_i)\right]^{-\frac{1}{\pi}(\delta_{i+1}-\delta_i)(2a_i\delta_i+b_i)} d\xi + B$$

A suitably small element is the largest possible element that can be written in the form of Equation (5). Practically, for smooth surfaces this element becomes larger and the number of such elements decreases and hence, the speed is enhanced.

Defining $\bar{\theta}_i$ to be the slope of the line connecting two points i and $i+1$, we can write:

$$\bar{\theta}_i = a_i \left(\frac{\delta_{i+1} + \delta_i}{2} \right)^2 + b_i \frac{\delta_{i+1} + \delta_i}{2} + c_i \tag{6}$$

We also have

$$\theta_{i+1} = a_i \delta_{i+1}^2 + b_i \delta_{i+1} + c_i \tag{7}$$

From (5), (6) and (7), a_i, b_i and c_i and hence, the mapping function is determined in terms of δ_i. An iterative procedure is needed to determine δ_i. For the initial values, we can set

$$x_i^{(0)} = u_i, \quad (i = 1, \ldots, N)$$

Then, we set the following rules for $x_i^{(k)}$ to converge:

$$\begin{aligned} x_{i+1}^{(k+1)} - x_i^{(k+1)} &= \left(x_{i+1}^{(k)} - x_i^{(k)} \right) \frac{\left| w_{i+1}^{(k)} - w_i^{(k)} \right|}{|w_{i+1} - w_i|} \\ i &= 1, \ldots, n-1, n+1, \ldots, N-1 \\ x_{n+1}^{(k+1)} - x_1^{(k+1)} &= \left(x_{n+1}^{(k)} - x_1^{(k)} \right) \frac{\left| w_{n+1}^{(k)} - w_1^{(k)} \right|}{|w_{n+1} - w_1|} \end{aligned}$$

w_i is the correct value of the discretization point on the curve. In each step, $w_i^{(k)}$ is evaluated from known $x_i^{(k)}$ and the iterative procedure is continued till the error tolerance for $w_i^{(k)}$ (compared with its correct value w_i) satisfies a predefined goal. Regardless of the number of discretization points, this iterative procedure converges after a few ten iterations. Note that two degrees of freedom are used to map $-\infty$ and $+\infty$ to the left- and right-ends of the infinite curve, respectively. One degree of freedom is remained [11], so we assume $x_1 = u_1$ which is a fixed value. A and B are used to fix the positions of w_1 and w_N. In each iteration step, an integration is needed to obtain $w_i^{(k)}$. Since there is a singularity in the integrand when $\xi = \delta$, compound Gauss-Jacobi quadrature is a preferred method for integration. The detailed integration method is described in [11]. We implemented the integration procedure in MATLAB.

3. VERIFICATION AND DISCUSSION

As shown in Figure 1, the rectangular patch antenna on a surface with parabolic cross-section is considered. The substrate dielectric constant and thickness are $\varepsilon_r = 2.2$ and $h = 1.588\,\text{mm}$, respectively. The conformal patch dimensions are $W = 12\,\text{mm}$, $W_0 = 0.3\,\text{mm}$, $s = 0.1\,\text{mm}$, $L = 9.06\,\text{mm}$ and $y_0 = 3\,\text{mm}$. SCT is used to map a straight planar channel to a channel with parabolic cross-section in the interval $u\epsilon[0, L_w]$ and with the parallel-line extension elsewhere. Assume that the patch is located on the parabola $v = au^2$ (u and v are in mm). For each curvature factor a, a planar patch antenna is resulted after mapping, which is designed and simulated very fast. In this section the methods used to generate plots are as follows: i) *DA* (Direct Approach): Full-wave simulation of the parabolic structure in CST which is a difficult and time-consuming task, ii) $CM + CST$ (Conformal Mapping + CST): Transforming the parabolic structure to a planar one and then full-wave simulation of the planar antenna in CST, iii) $CM + TL$ *Model* (Conformal Mapping + Transmission-Line Model): Transforming the parabolic structure to a planar one and then using the transmission-line model of the planar antenna (described in [16]) to find the input impedance, iv) CM+*Cavity Model* (Conformal Mapping + Cavity Model): Transforming the parabolic structure to a planar one and then using cavity model of the planar antenna (described in [16]) to find the radiation-pattern. In this work, we used a maximum number of 52 segments in order to make the modified SCT method converge. When the run takes place on a corei7 PC with 12 Gigabytes RAM, the $CM + CST$, $CM + TL$ *Model*, and CM+ *Cavity Model* methods are about 8, 22 and 22 times faster than *DA*, respectively.

Figure 3 shows the input impedance of the curved patch antenna in terms of the curvature factor a. The curvature increases input impedance by about $6.5|a|$. This figure shows the verification of CM+CST and CM+TL *Model* methods by *DA*. Figures 4(a) and 4(b) show input impedance and VSWR in terms of frequency for two cases $a = 0$ (when the patch antenna is exposed to no curvature) and $a = -0.2$. As Figure 4 illustrates, the *DA* and $CM + CST$ methods agree well. Figure 4(a) shows the effect of curvature on real- and imaginary parts of the input impedance of the patch antenna seen from the feed line. Figure 4(b) shows the effect of curvature on VSWR. All in all, curvature increases VSWR and deteriorates return-loss. As seen, there is a very small change in the resonance frequency (f_r). This can be described by the proposed theory. The patch cavity model works in TM_{010} mode and from [16], f_r is mostly dependent on L and not on

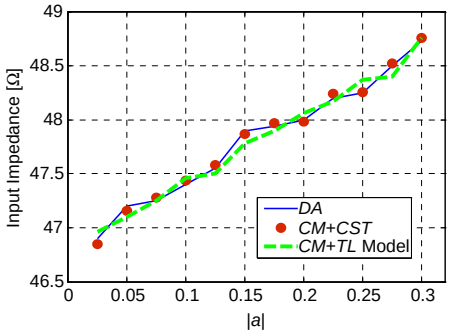

Figure 3. Input impedance in terms of $|a|$, computed by DA, $CM + CST$ and $CM + TL$ model methods.

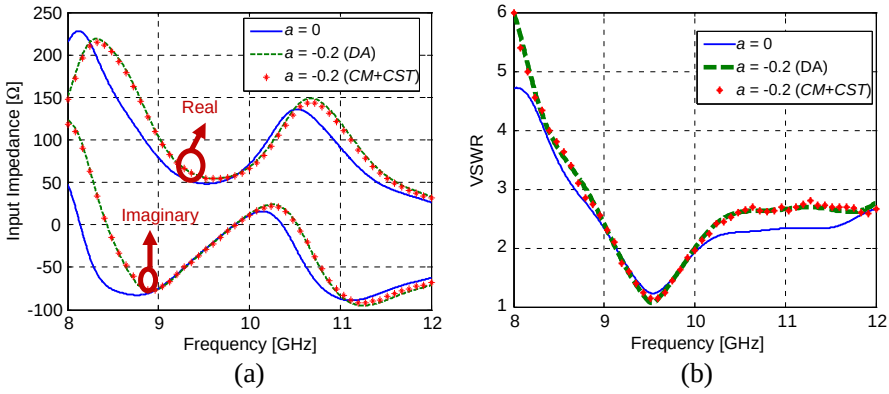

Figure 4. (a) Input impedance and (b) VSWR in terms of frequency, when the patch is exposed to no curvature and when it is curved (DA and $CM + CST$ methods).

W (ignoring the fringing effect). The SCT maps the two dimensional cross-section and hence affects W, whereas, it keeps L unchanged. Hence, there should be no change in f_r. Considering fringing effect, f_r changes a bit, since in this case it depends on W. Note that both input impedance and VSWR are functions of the characteristic impedance (Z_0) of the transmission line (TL). Since conformal mapping preserves Z_0 [14], it also preserves input impedance and VSWR of a TL.

Since the patch antenna radiating slots are the curved slots, the conformal map is expected to preserve the radiation pattern of the patch antenna. Note that conformal mapping preserves scalar quantities in z- and w-planes. In w-plane, the radiation-pattern

is a scalar quantity (electric-field magnitude) around a very large circle. This quantity is preserved when transforming z-plane to w-plane. However, the shape to be mapped to the far-field circle is not necessarily a circle but a very large shape. For any angular location, this shape is confined between two large far-field circles which demonstrate the same far-field behavior at that angular location (far-field radiation-patterns on those circles are independent of the distance from the antenna). Hence, conformal mapping preserves the far-field radiation-patterns verified in Figures 5 and 6. Figure 5(a) and Figure 5(b) show E- and H-plane radiation patterns for different values of a. As seen, the two $CM + CST$ and DA methods agree well. As the curvature factor (a) increases, the conformal patch antenna covers a wider range of angles in H-plane, however, no change occurs for that in E-plane (Figure 1(a)). Hence, H-plane radiation pattern becomes broader but the E-plane beamwidth is expected to remain unchanged. On the other hand, based on the proposed method, as a increases, the mapped planar patch attains a smaller width (W). Based on cavity model formulas described in [16] for a planar rectangular patch antenna, change in W does not affect E-plane beamwidth but as W decreases, H-plane pattern becomes broader. Hence, both physical and analytical explanations of this phenomenon agree well with each other. Figure 6 compares $CM+$ *Cavity Model* and DA methods for E- and H-plane radiation-patterns. As it is clear, the patch antenna cavity model can't predict back lobes. As Figure 2 shows, theoretically both

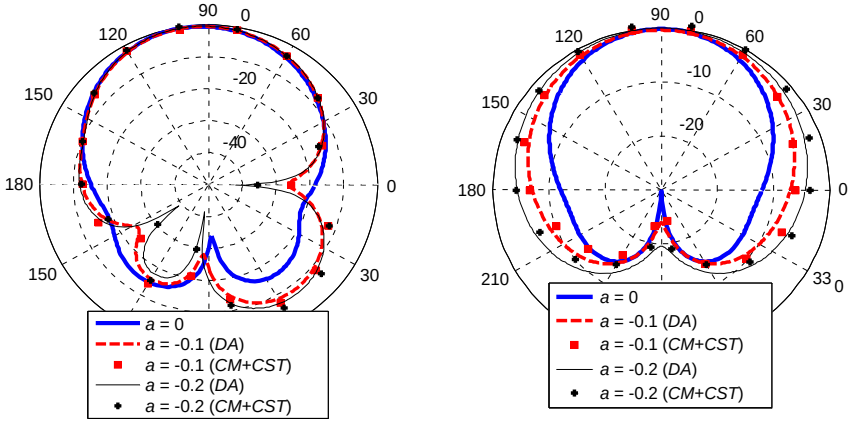

Figure 5. Radiation patterns of patch antenna for different curvatures obtained by DA and $CM + CST$ methods. (a) E-plane. (b) H-plane.

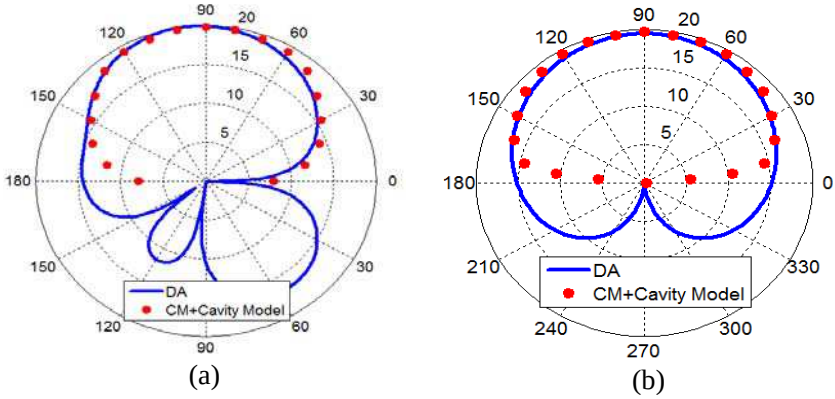

Figure 6. Radiation patterns of patch antenna obtained for $a = -0.2$, by DA and $CM + Cavity$ model methods. (a) E-plane. (b) H-plane.

conformal and mapped planar structures are assumed to be infinitely long and hence have no back lobes. However, for numerical calculations the infinite intervals are truncated and hence the antennas have finite lengths and finite ground-planes which results in back-lobes. There is almost agreement between the two methods in the main lobes.

4. CONCLUSION

A general cross-section for a conformal structure on a dielectric substrate is a region (sometimes elongated) with curved boundaries. In this paper, the Schwarz-Christoffel mapping is modified to deal with elongated regions with curved boundaries. Segmentation of the curved boundary is used to evaluate SCT numerically. Each segment is approximated by a second degree polynomial. A relatively small number of segments make the approaches converge for smooth curves and yield both SCT and inverse SCT numerically. This theory is verified by computing the input impedance, VSWR and radiation patterns of a patch antenna on a parabolic surface and comparing them with CST full-wave simulator results.

REFERENCES

1. He, M. and X. Xu, "Closed-form solutions for analysis of cylindrically conformal microstrip antennas with arbitrary radii," *IEEE Trans. Antennas Propag.*, Vol. 53, No. 1, 518–525, Jan. 2005.

2. Amendola, G., "Application of Mathieu functions to the analysis of radiators conformal to elliptic cylindrical surfaces," *Journal of Electromagnetic Waves and Applications*, Vol. 13, No. 8, 1103–1120, 1999.
3. Yuan, N., X. C. Nie, Y. B. Gan, T. S. Yeo, and L. W. Li, "Accurate analysis of conformal antenna arrays with finite and curved frequency selective surfaces," *Journal of Electromagnetic Waves and Applications*, Vol. 21, No. 13, 1745–1760, 2012.
4. Dib, N. and T. Weller, "Finite difference time domain analysis of cylindrical coplanar waveguide circuits," *Journal of Electromagnetic Waves and Applications*, Vol. 87, No. 9, 1083–1094, 2000.
5. Revuelto, I. G., L. E. G. Castillo, F. S. Adana, M. S. Palma, and T. K. Sarkar, "A novel hybrid FEM high-frequency technique for the analysis of scattering and radiation problems," *Journal of Electromagnetic Waves and Applications*, Vol. 18, No. 7, 939–956, 2004.
6. Arakaki, D. Y., D. H. Werner, and R. Mittra, "A technique for analyzing radiation from conformal antennas mounted on arbitrarily-shaped conducting bodies," *Proc. IEEE International Symp. on Antennas and Propag.*, Vol. 1, 10–13, 2000.
7. Macon, C. A., K. D. Trott, and L. C. Kempel, "A practical approach to modeling doubly curved conformal microstrip antennas," *Journal of Electromagnetic Waves and Applications*, Vol. 17, No. 8, 1161–1163, 2003.
8. Hosseini, K. and Z. Atlasbaf, "Design of a cylindrical CRLH leaky-wave antenna using conformal mapping," *IEEE International Symp. on Telecommun. (IST2012)*, Tehran, 2012.
9. Kadi, Z. and A. Rockwood, "Conformal maps defined about polynomial curves," *Computer Aided Geometric Design*, Vol. 15, 323–337, 1998.
10. Driscoll, T. A., "A non-overlapping domain decomposition method for Symm's equation for conformal mapping," *Society for Industrial and Applied Mathematics*, Vol. 36, No. 3, 922–934, 1999.
11. Howell, L. H., "Computation of conformal maps by modified Schwarz-Christoffel transformation," Ph.D. Dissertation, Dept. Math., Massachussets Inst. of Technology, MA, 1990.
12. Davis, R. T., "Numerical methods for coordinate generation based on Schwarz-Christoffel transformation," *AIAA Computational Fluid Dynamics Conference*, Vol. A79-45251, 180–194, 1979.
13. Akan, V. and E. Yazgan, "Quasi-static solutions of multilayer

elliptical, cylindrical coplanar striplines and multilayer coplanar striplines with finite dielectric dimensions-asymmetrical case," *IEEE Trans. Antennas Propag.*, Vol. 53, No. 12, 3681–3686, Dec. 2005.

14. Nguyen, C., *Analysis Methods for RF, Microwave, and Millimeter-wave Planar Transmission-line Structures*, Chapter 5, John Wiley & Sons, New York, 2000.
15. Brown, J. W. and R. V. Churchill, *Complex Variables and Applications*, 8th Edition, Chapter 11, Mc-Graw Hill, New York, 2004.
16. Balanis, C. A., *Antenna Theory, Analysis and Design*, 3rd Edition, Chapter 14, John Wiley, New Jersey, 2005.